Comparative analysis of *Wolbachia* maternal transmission and localization in host ovaries

Michael T.J. Hague[1,#], Timothy B. Wheeler[2], Brandon S. Cooper[2]

[1]Biology Department
University of Scranton
Scranton, Pennsylvania, USA

[2]Division of Biological Sciences
University of Montana
Missoula, Montana, USA

[#]Corresponding Author
michael.hague@scranton.edu

ABSTRACT

Many insects and other animals carry microbial endosymbionts that influence their reproduction and fitness. These relationships only persist if endosymbionts are reliably transmitted from one host generation to the next. *Wolbachia* are maternally transmitted endosymbionts found in most insect species, but transmission rates can vary across environments. Maternal transmission of *w*Mel *Wolbachia* depends on temperature in natural *Drosophila melanogaster* hosts and in transinfected *Aedes aegypti*, where *w*Mel is used to block pathogens that cause human disease. In *D. melanogaster*, *w*Mel transmission declines in the cold as *Wolbachia* become less abundant in host ovaries and at the posterior pole plasm (the site of germline formation) in mature oocytes. Here, we assess how temperature affects maternal transmission and underlying patterns of *Wolbachia* localization across 10 *Wolbachia* strains diverged up to 50 million years—including strains closely related to *w*Mel—and their natural *Drosophila* hosts. Many *Wolbachia* maintain high transmission rates across temperatures, despite highly variable (and sometimes low) levels of *Wolbachia* in the ovaries and at the developing germline in late-stage oocytes. Identifying strains like closely related *w*Mel-like *Wolbachia* with stable transmission across variable environmental conditions may improve the efficacy of *Wolbachia*-based biocontrol efforts as they expand into globally diverse environments.

KEYWORDS: *w*Mel, *Drosophila*, host-microbe interaction, vertical transmission

INTRODUCTION

Microbes form diverse relationships with host organisms that span the tree of life, including animals, plants, and protists. Endosymbiosis is an especially close relationship where microbes occupy eukaryotic host cells. Heritable endosymbionts are particularly common in insects[1–3], and these relationships alter fundamental aspects of host biology, including reproduction[4,5], protection for natural enemies[6–9], and nutrient acquisition[10–12].

Many endosymbionts rely on vertical-maternal transmission to spread and persist in insect populations[13–15]. In obligate relationships, these endosymbionts must be maternally transmitted to ensure host survival (e.g., *Buchnera* and aphids[16]). For facultative endosymbionts like *Wolbachia*, imperfect maternal transmission decreases the prevalence of *Wolbachia*-positive individuals within the host population each generation[17–21]. Thus, maternal transmission is a fundamental determinant of how endosymbionts spread, persist, and evolve in host populations[17,22,23]. In addition, endosymbiont-based programs to control human diseases[24–26] and agricultural pests[27,28] explicitly depend on efficient maternal transmission of *Wolbachia* in transinfected insect vectors and pest populations. This includes introducing the virus-blocking *w*Mel *Wolbachia* strain from *Drosophila melanogaster* into mosquito populations to block dengue and other arboviruses on multiple continents[29–32]. Nonetheless, it is largely unknown why maternal transmission may break down under certain circumstances, especially for non-model systems[15,21,33–36].

Maternal transmission is predicted to depend on endosymbiont density (titer) in female reproductive tissues, and specifically at the site of germline formation during oogenesis[14]. In insects, endosymbionts often achieve vertical transmission by occupying the female ovaries. Endosymbionts are observed in germline stem cells in female hosts where they maintain a tight association with the germline throughout oogenesis, thereby ensuring a germline-to-germline route of vertical transmission through the host matriline[14,15,36,37]. In a more circuitous route, some endosymbionts may also colonize the germline from neighboring somatic cells via cell-to-cell migration through a soma-to-germline route of transmission[4,14,15,38,39]. Our canonical understanding of these cellular processes—and their contributions to maternal transmission—are based almost entirely in the context of standard laboratory conditions where maternal transmission rates are near perfect or perfect[18,20,21,40]. However, maternal transmission of facultative endosymbionts is often imperfect in natural host populations[19,20,41,42] and the cellular

52 processes that lead to transmission breakdown under natural conditions are generally
53 unresolved[21,36]. Understanding why transmission breaks down under certain conditions is critical
54 for predicting endosymbiont spread in nature and improving *Wolbachia*-based biocontrol
55 programs[25,33,34,43].

56 Maternally transmitted *Wolbachia* are the most common endosymbionts on earth,
57 associating with about half of all insect species, as well as other arthropods and nematodes[4,44–46].
58 *Wolbachia* are primarily maternally (vertically) transmitted via the host germline within host
59 species; although, host switching via horizonal transfer between host species is common on
60 evolutionary timescales[47–54]. *Wolbachia* generally form facultative relationships (from the host
61 perspective) in insects, with some individuals in the host population that do not carry *Wolbachia*
62 due to imperfect maternal transmission. Maternal transmission is perhaps the most important
63 determinant of *Wolbachia* prevalence in host populations: theory demonstrates that *Wolbachia*
64 frequency dynamics and equilibria are approximated by the degree of imperfect maternal
65 transmission (μ), the relative fitness (e.g., fecundity) of females with *Wolbachia* (F), and the
66 strength of *Wolbachia*-induced cytoplasmic incompatibility (s_h)[17,55]. Some *Wolbachia* strains
67 (e.g., *w*Ri in *D. simulans*) cause cytoplasmic incompatibility (CI), a crossing incompatibility that
68 generates a frequency-dependent advantage for females with *Wolbachia*[5,56].

69 The prevalence of different *Wolbachia* strains varies widely among host systems, which
70 may be partially explained by differences in maternal transmission rates. For instance, the strong
71 CI-causing *w*Ri strain is observed at high frequencies in global *D. simulans* populations[17,18,57],
72 whereas the weak CI-causing *w*Mel strain is found at intermediate, fluctuating frequencies in *D.*
73 *melanogaster*[58]. *w*Ri frequencies can be plausibly explained by strong CI that causes spread to
74 high frequencies, whereas lower, variable *w*Mel frequencies can be plausibly explained by
75 maternal transmission breakdown as temperatures decrease, in addition to a minimal influence of
76 CI[21]. The thermal sensitivity of maternal transmission may be a feature of *w*Mel, given that heat
77 stress also reduces *w*Mel transmission in transinfected *Aedes aegypti* hosts[33,34,43]. Identifying
78 *Wolbachia* variants that are efficiently transmitted across environmental conditions could
79 potentially contribute to improving the efficacy of *Wolbachia* based biocontrol of human
80 diseases and agricultural pests[25,26].

81 What might underlie variable maternal transmission rates? Maternal transmission
82 breakdown is predicted to stem from reductions in *Wolbachia* abundance and localization

83 throughout host development and specifically at the critical stages of oogenesis thought to
84 facilitate germline-to-germline maternal transmission[14,15,21,36,59–63]. *w*Mel cells are present in the
85 germline stem cells of adult females, and over the course of oogenesis, *w*Mel localize via
86 kinesin-mediated transport to the pole plasm—the site of germline formation—at the posterior
87 cortex of the developing oocyte. In late oogenesis (stage 10), *w*Mel *Wolbachia* display a pattern
88 of posterior localization in oocytes, which is considered to be a key step in the process of
89 germline-to-germline maternal transmission under standard laboratory conditions[14,50,59–63]. In
90 support of this, we recently demonstrated that declining *w*Mel transmission in the cold covaries
91 with a significant reduction in cellular *Wolbachia* abundance at the posterior cortex of stage 10
92 oocytes, which can plausibly explain why maternal transmission is thermally sensitive[21].
93 Outside of the *w*Mel strain, it is unclear how temperature influences *Wolbachia* maternal
94 transmission and posterior localization in stage 10 oocytes for other diverse *Wolbachia*-host
95 associations[15,20]. Under standard 25°C conditions, divergent *Wolbachia* strains exhibit highly
96 variable patterns of localization to the pole plasm at the posterior cortex of stage 10 oocytes of
97 *Drosophila* species, deviating from our canonical understanding of *w*Mel[15]. These patterns range
98 from strongly localized (e.g., *w*Ana in *D. anannassae*) to a complete lack of localization (e.g.,
99 *w*Tri in *D. triauraria*) at the site of germline formation. Some strains, particularly the divergent
100 B-group *w*Mau strain, also exhibit evidence for an alternative soma-to-germline route of
101 transmission, whereby *Wolbachia* in somatically derived follicle cells may invade the oocyte via
102 cell-to-cell migration. It is entirely unknown whether the diverse localization patterns of these
103 *Wolbachia* strains influence rates of maternal transmission and/or are sensitive to thermal
104 perturbation like *w*Mel.
105 Here, we examine temperature effects on *Wolbachia* maternal transmission and
106 localization in host tissues across 10 divergent *Wolbachia* strains naturally found in eight
107 *Drosophila* host species within the *melanogaster* species group (Figure 1, Table S1). These
108 *Wolbachia* comprise nine A-group *Wolbachia*—including closely related *w*Mel-like strains
109 (*w*Mel, *w*MelCS, *w*Seg in *D. seguyi*, and *w*Cha in *D. chauvacae*) and closely related *w*Ri-like
110 strains (*w*Ri, *w*Ana in *D. ananassae*, *w*Aura in *D. auraria*, and *w*Tri in *D. triauraria*)[20,51,53]—and
111 divergent B-group *w*Mau in *D. mauritiana* that diverged up to 46 million years ago from the
112 other A-group strains[40]. We reared flies at 25° and 20°C and then measured maternal
113 transmission rates in conjunction with *Wolbachia* densities (titer) at the tissue level in female

114 ovaries and the remaining somatic tissues. We then used confocal microscopy to examine how
115 temperature impacts the cellular abundance of *Wolbachia* at the site of germline formation at the
116 posterior cortex of stage 10 oocytes during oogenesis. Our results reveal diverse patterns of
117 localization in ovary tissues and late-stage oocytes that are temperature-dependent, but only
118 weakly predictive of maternal transmission rates. We also identify *Wolbachia* strains that are
119 transmitted efficiently regardless of temperature.
120
121 **RESULTS**
122 We estimated the mean rate of maternal transmission (± BC_a confidence intervals) for
123 each *Wolbachia*-host genotype at 25° and 20°C by pairing individual virgin females with
124 *Wolbachia*-free males (see Methods), allowing the females to lay for eight days, and then
125 measuring maternal transmission ($1 - \mu$) to the newly emerged offspring of each subline (Figure
126 2, Table S2)[20,21]. The final dataset comprised 365 F0 females and 3,612 F1 offspring. Overall, we
127 found a significant interaction effect between the *Wolbachia*-host genotype and temperature
128 (GLMM LRT, $\chi^2_{(9)} = 23.49$, $P = 0.005$), such that temperature effects on maternal transmission
129 varied depending on the *Wolbachia*-host genotype. For most *Wolbachia*-host genotypes, mean
130 rates of maternal transmission were perfect (e.g., *w*Ri-*D. simulans*) or near-perfect (e.g., *w*Mel-
131 like *w*Seg-*D. seguyi*) and invariant across the two temperatures (Figure 2, Table S3), with the
132 exception of a few specific *Wolbachia*-host genotypes. Maternal transmission of *w*Mel by *D.*
133 *melanogaster* ($W = 251.5$, $P = 0.003$) and *w*Aura by *D. auraria* ($W = 154$, $P = 0.038$) decreased
134 significantly at 20°C; although, *w*Mel experienced a much greater decline in the average rate of
135 transmission (14.9%) than *w*Aura (2.8%). In contrast, B-group *w*Mau transmission by *D.*
136 *mauritiana* increased slightly by 3.4% in the cold at 20°C ($W = 117$, $P = 0.019$). Notably, our
137 analysis also revealed a significant effect of sex (GLMM LRT, $\chi^2_{(1)} = 63.71$, $P < 0.001$), whereby
138 rates of maternal transmission tended to be lower to female offspring than males (Table S2). This
139 finding is consistent with our previous findings for *w*Mel[21] and the *w*Mel-like *w*Yak strain in *D.*
140 *yakuba*[20], but counter to theoretical expectations that selection should favor faithful transmission
141 to female offspring[64,65].
142 To test for temperature effects on *Wolbachia* at the tissue level, we dissected out the
143 ovaries from a subset of the same F0 females assessed for maternal transmission above ($N =$
144 183). For this analysis we used qPCR to measure *Wolbachia* densities in the ovaries and the

145 remaining somatic carcass tissue (Figure 3). We found a significant interaction effect between
146 the *Wolbachia*-host genotype and temperature on *Wolbachia* density in ovaries (Two-way
147 ANOVA; $F_{(9,161)} = 4.286$, $P < 0.001$) and the remaining carcasses ($F_{(9,161)} = 10.612$, $P < 0.001$),
148 such that temperature effects on *Wolbachia* density varied depending on the *Wolbachia*-host
149 genotype. While we uncovered considerable variation depending on the *Wolbachia*-host
150 genotype and temperature, *Wolbachia* ovary densities generally tended to decline at 20°C for the
151 majority of systems (Figure 3, Table S4). Five of the *Wolbachia* strains (*w*Mel, *w*Ri, *w*Ana, *w*Ha,
152 and *w*Mau) decreased in density in the ovaries in the cold. In contrast, carcasses exhibited
153 variation in the directionality of changes in *Wolbachia* density. *w*Mel, *w*MelCS, *w*Seg, and
154 *w*Aura densities decreased significantly in the cold, whereas *w*Cha and *w*Mau significantly
155 increased. *w*Cha densities in carcasses were roughly an order of magnitude lower than all other
156 strains, regardless of temperature, suggesting a relatively high degree of localization to the
157 ovaries. *w*Mel, the strain that experienced the most dramatic decline in transmission in the cold
158 (Figure 2), was also the only *Wolbachia* strain that experienced a significant decline in
159 *Wolbachia* density in both the ovaries and the carcasses in the cold. This included a particularly
160 large decline in density in the carcasses (a 4.7-fold reduction) compared to the other strains.
161 For the three *Wolbachia*-host systems with temperature-dependent transmission (*w*Mel,
162 *w*Aura, and *w*Mau), we also tested for a correlation between transmission rates and *Wolbachia*
163 density in the ovaries and carcasses of the same individual females (Figure S1). Declining *w*Mel
164 transmission in the cold was significantly correlated with *Wolbachia* density in the ovaries
165 (Spearman's $\rho = 0.537$, $P = 0.022$), but not the carcasses ($\rho = 0.392$, $P = 0.108$), providing
166 additional support that reduced *w*Mel density in reproductive tissues contributes to transmission
167 breakdown in the cold. Maternal transmission of *w*Aura by *D. auraria* did not strongly correlate
168 with *w*Aura density in the ovaries ($\rho = -0.244$, $P = 0.380$) or the carcasses ($\rho = 0.035$, $P = 0.902$).
169 Finally, increasing maternal transmission of *w*Mau by *D. mauritiana* in the cold did not correlate
170 with *w*Mau density in the ovaries ($\rho = -0.119$, $P = 0.649$), but was significantly correlated with
171 density in the carcasses ($\rho = 0.549$, $P = 0.022$).
172 Finally, we examined how temperature impacts cellular *Wolbachia* abundance at the site
173 of germline formation in stage 10 oocytes during host oogenesis. At this stage, *w*Mel *Wolbachia*
174 localization at the posterior cortex of the oocyte is considered to be a critical step in the process
175 of germline-to-germline *Wolbachia* maternal transmission[14,15,21,36,59–63]. We imaged a total of 283

176 stage 10 oocytes from eight-day-old females reared at the two different temperatures and
177 quantified cellular *Wolbachia* abundance (measured as corrected total cell fluorescence; CTCF)
178 in the whole oocytes, the posterior region, and the posterior cortex (Figure S2)[14,15,21]. We defined
179 the posterior region as the posterior 1/8th portion of the oocyte and the posterior cortex as the
180 narrow cortical region of Vasa expression (a germline protein component)[15,63]. For the sake of
181 clarity and consistency with the literature, we refer to our *Wolbachia* quantifications with
182 confocal microscopy here as "cellular *Wolbachia* abundance" in oocytes, as opposed to the
183 quantification of "*Wolbachia* density" at the tissue level using qPCR (described above).
184 Cellular *Wolbachia* abundance in whole oocytes (Two-way ANOVA; $F_{(9,263)} = 2.9$, $P =$
185 0.003), at the posterior region ($F_{(9,263)} = 4.16$, $P < 0.001$), and at the posterior cortex ($F_{(9,263)} =$
186 2.41, $P = 0.012$) depended on significant two-way interactions between the *Wolbachia*-host
187 genotype and temperature. As with *Wolbachia* density, cellular *Wolbachia* abundance in oocytes
188 varied considerably depending on the *Wolbachia*-host genotype and temperature (Figures 4, S3).
189 The cellular abundance of six of the *Wolbachia* strains (*w*MelCS, *w*Seg, *w*Ana, *w*Aura, and *w*Tri,
190 and *w*Ha) declined significantly throughout whole oocytes in the cold (Table S5). Temperature
191 affected fewer strains (only *w*Mel, *w*MelCS, *w*Ri, and *w*Aura) at the posterior region and the
192 posterior cortex, the location of the developing germline. *w*Mel and *w*Aura, the two strains
193 transmitted at significantly lower rates in the cold, both declined significantly in abundance in
194 the posterior oocyte region ($W = 113$, $P = 0.015$; $W = 172$, $P = 0.041$). *w*Mel cellular abundance
195 also significantly declined at the posterior cortex ($W = 122$, $P = 0.002$). Interestingly, *w*MelCS
196 also exhibited a significant decline in cellular abundance in the posterior region ($W = 203$, $P <$
197 0.001) and the cortex ($W = 205$, $P < 0.001$), despite the fact that *w*MelCS transmission by *D.*
198 *melanogaster* was not altered in the cold (Figure 2). This can perhaps be explained by the fact
199 that, of all 10 strains, *w*MelCS had the highest cellular abundance at the posterior region and
200 cortex, regardless of temperature. Finally, *w*Ri was perfectly transmitted by *D. simulans* at both
201 temperatures, but *w*Ri abundance increased at the oocyte posterior region ($W = 45$, $P = 0.004$)
202 and the cortex ($W = 49$, $P = 0.008$) in the cold. Also of note, *w*Aura and *w*Tri occurred at
203 particularly low abundances in the oocyte posterior region and the posterior cortex, regardless of
204 temperature, despite both being transmitted at relatively high rates by their female hosts ($1 - \mu >$
205 0.967).

206 Our analyses revealed that the diverse *Wolbachia* strains and *Drosophila* host species
207 exhibit extensive variation in *Wolbachia* density in host tissues (Figure 3) and abundance in host
208 oocytes (Figure 4). We hypothesized that this diversity may be explained by factors in the
209 *Wolbachia* or host genomes (or both). If so, we expect closely related *Wolbachia* strains (or host
210 species) to exhibit similar patterns of *Wolbachia* localization in host tissues[15,66,67]. We used the
211 *Wolbachia* and host trees (Figure 1) to test whether patterns of *Wolbachia* localization in tissues
212 and oocytes exhibit phylogenetic signal using Pagel's λ[68]. A value of 1 is consistent with trait
213 evolution that entirely agrees with the *Wolbachia* (or host) phylogeny, suggesting factors in the
214 *Wolbachia* genome (or host) contribute to *Wolbachia* localization patterns (i.e., strong
215 phylogenetic signal). In contrast, a value of 0 is consistent with trait evolution that occurs
216 independently of phylogenetic relationships[68,69]. We found no evidence that *Wolbachia* density
217 in the ovaries and carcasses, nor cellular abundance in the oocytes, exhibit phylogenetic signal
218 on the *Wolbachia* phylogeny (Table S6, Figure S4), implying that factors in the *Wolbachia*
219 genome do not account for observed diversity. In contrast, we found that *Wolbachia* density in
220 the ovaries at 25°C exhibits strong, significant phylogenetic signal on the host phylogeny (λ =
221 1.000, P = 0.001), implying that factors in the host genome may help determine observed
222 diversity of *Wolbachia* densities in host ovaries. In this instance, related species in the *montium*
223 species group tended to have lower *Wolbachia* densities in the ovaries relative to the
224 *melanogaster* subgroup (see Figure S5). Divergent *D. ananassae* also had a higher *Wolbachia*
225 density than all the other host species. We also found that cellular *Wolbachia* abundance in the
226 oocyte posterior region (λ = 1.000, P = 0.037) and the posterior cortex (λ = 1.000, P = 0.036)
227 exhibited a significant signature of phylogenetic signal at 20°C on the host phylogeny. This
228 pattern is largely driven by the relatively low abundance of *Wolbachia* in the posterior oocytes of
229 the two closely related species *D. triauraria* and *auraria*.
230
231 **DISCUSSION**
232 Maternal transmission rates are a key determinant of *Wolbachia* prevalence in host
233 populations[17,55]. For many *Wolbachia* strains and host species, we found that maternal
234 transmission is generally high and stable across two ecologically relevant temperatures, 25º and
235 20ºC, that flies are likely to experience in natural environments[21,70]. Two *Wolbachia* strains
236 (*w*Aura and B-group *w*Mau) exhibited minor temperature-dependent changes in transmission,

but *w*Mel stood out with a relatively large decrease in transmission as temperature dropped from 25° to 20°C (Figure 2). Maternal transmission is generally expected to depend on *Wolbachia* density in host reproductive tissue[20,34,43,71], and specifically within developing oocytes[14,15,21,36,59–63]. Our analyses uncovered considerable, significant variation in *Wolbachia* densities at the tissue level and cellular abundances in oocytes, which also often varied depending on temperature. With the exception of *w*Mel, *Wolbachia* densities in ovary tissue generally did not predict maternal transmission rates (Figures 3, S1). In stage 10 oocytes, declines in the cellular abundance of *w*Mel and *w*Aura at the posterior region coincided with declining transmission in the cold (Figure 4), but the *w*MelCS and *w*Ri strains also experienced changes in cellular abundance that did not correlate with differences in maternal transmission. Together, these results suggest that maternal transmission rates cannot be accurately predicted from measurements of *Wolbachia* quantities in ovary tissue or late-stage oocytes. First, we explore the diverse patterns of *Wolbachia* localization in relation to maternal transmission in our comparative analyses. Then, we examine why maternal transmission of some strains, particularly *w*Mel, may be impacted by temperature.

At the tissue level, we found that *Wolbachia* densities in the ovaries generally did not predict rates of maternal transmission, with the exception of *w*Mel. *w*Mel density in the ovaries of individual females was tightly correlated with declining transmission rates in the cold (ρ = 0.537, Figure S1). Temperature did not alter *w*Aura density in the ovaries despite declining *w*Aura transmission in the cold, and *w*Mau density counterintuitively declined at 20°C despite transmission increasing. Other strains (e.g., *w*Ri and *w*Ha in *D. simulans*) experienced large declines in *Wolbachia* ovary density at 20°C with no impact on maternal transmission. *Wolbachia* densities in the remaining somatic carcass tissue also generally did not predict declining transmission in the cold; however, *w*Mau densities in the carcasses of individual females were strongly correlated with increased transmission in the cold (ρ = 0.549; discussed further below). Notably, *w*Cha was exceptional in terms of its very low density in carcass tissue relative to other strains, despite perfect transmission at both temperatures. Changes to host ploidy in the ovaries could plausibly contribute to the observed differences in relative *Wolbachia* density[72]; however, we did not find evidence for significant changes in host gene copy number in the ovaries across temperature treatments (Figure S6).

267 At the cellular level, *Wolbachia* abundance in stage 10 oocytes may help explain why
268 *w*Mel and *w*Aura experienced declining transmission in the cold. Many strains experienced
269 declines in cellular *Wolbachia* abundance throughout the whole oocyte at 20°C (Figure 4a), but
270 this was generally unrelated to transmission rates. *w*Mel was one of the few strains that had a
271 significant reduction in cellular abundance at the posterior region (Figure 4b) and cortex (Figure
272 4c), the site of germline formation. Similarly, *w*Aura had a reduced abundance in the posterior
273 region at 20°C (but not at the cortex). *w*MelCS (closely related to *w*Mel) was the only additional
274 strain with significant reductions in abundance at the posterior region and the cortex. However,
275 *w*MelCS occurred at a much higher absolute abundance than *w*Mel, *w*Aura, and all other
276 *Wolbachia* strains, which may explain why transmission remained high at 20°C (discussed
277 further below). We conjecture that there is presumably a minimum cellular abundance required
278 for efficient transmission, and *Wolbachia* strains like *w*MelCS that are generally very abundant
279 are less likely to fall below this threshold. A reduction in cellular abundance at the oocyte
280 posterior implies that fewer *Wolbachia* cells will be incorporated into the germline later during
281 host development, perturbing germline-to-germline maternal transmission[21]. The fact that both
282 *w*Mel and *w*Aura had significantly reduced abundances in the posterior region at 20°C implies
283 that perturbations of cellular *Wolbachia* abundance in this region may help explain why some
284 *Wolbachia* strains have reduced transmission in the cold. *w*Ri was the only other *Wolbachia*
285 strain with an altered abundance at the oocyte posterior region and cortex, but cellular abundance
286 increased at 20°C. This may help explain why maternal transmission of *w*Ri remained perfect at
287 20°C. Interestingly, a low absolute abundance of *Wolbachia* was not necessarily associated with
288 declining maternal transmission. The *w*Tri strain (closely related to *w*Aura) occurred at a lower
289 posterior abundance than all other strains, despite maintaining a high rate of transmission at both
290 temperatures.
291 It is important to note that our analysis of *Wolbachia* in ovary tissues and stage 10
292 oocytes of eight-day-old females represents only a snapshot of host development. Many other
293 unexplored factors may contribute to transmission rate variation. Other stages of development,
294 like embryogenesis, could also be involved in mediating maternal transmission. For instance,
295 temperature could impact *Wolbachia* localization at the newly formed germline of late
296 blastoderm and cellularized embryos, which could influence maternal transmission[15,60]. Cellular
297 *Wolbachia* abundance changes over the course of oogenesis and embryogenesis[15,61,72,73] and a

298 number of studies report complex, age-related changes in *Wolbachia* densities over the course of
299 the host's lifespan[74–81]. Maternal age and the order of egg-laying could also conceivably
300 influence *Wolbachia* transmission and densities in offspring[82]. Our work motivates future studies
301 on how temperature affects the distribution of *Wolbachia* in host tissues over the course of host
302 development in relation to maternal transmission.

303 Our comparative analysis highlights how *w*Mel seems to be especially susceptible to
304 cooling temperatures[21], which is consistent with our previous work suggesting the strain is less
305 prevalent in temperate host populations due to declining transmission in the cold[21,58]. In
306 transinfected mosquitoes, *w*Mel maternal transmission and densities are also more susceptible to
307 heat stress relative to another *Wolbachia* strain, *w*AlbB[25,26,33,34,43]. A number of factors could
308 plausibly help explain why *w*Mel maternal transmission is especially impacted by the cool
309 temperature, relative to other strains. At the tissue level, *w*Mel was the only *Wolbachia* we
310 examined that exhibited a significant decline in *Wolbachia* density in both the ovaries and the
311 carcasses at 20°C (Figure 3). Declining transmission was highly correlated with declining *w*Mel
312 density in the ovaries, plus *w*Mel stood out with a dramatic decline in *Wolbachia* density in
313 carcasses at 20°C compared to other strains. While *w*Mel is generally thought to follow a
314 germline-to-germline route of maternal transmission during oogenesis, our recent work and
315 others suggests that the strain may also rely on a soma-to germline mode of transmission[15,83,84].
316 *w*Mel *Wolbachia* are capable of cell-to-cell migration[84] and *w*Mel injected directly into the
317 abdomen of adult *D. melanogaster* females can migrate to and occupy the germline and follicle
318 stem cells[83]. The declines of *w*Mel densities throughout host tissues could potentially impact
319 routes of transmission originating in somatic tissue. At the cellular level, *w*Mel is also one of the
320 few strains (in addition to *w*Aura) to experience a decline in abundance at the posterior of stage
321 10 oocytes, which is expected to impact a germline-to-germline route of transmission. The
322 concurrent reduction in *Wolbachia* density in female tissues and oocytes may be a one-two
323 punch that impacts both soma- and germline-to-germline routes of *w*Mel transmission.

324 The juxtaposition between *w*Mel and *w*MelCS is interesting, because the two strains
325 diverged recently in only the last 3,000-14,000 years[85]. The *w*Mel and *w*MelCS strains we used
326 in our study are highly similar (0.007% third-position pairwise differences). Despite the close
327 relationship, *w*MelCS transmission was not impacted by temperature and the strain occurred at a
328 higher cellular abundance at the oocyte posterior than any of the other strains that we examined,

329 regardless of temperature. Some oocytes contained especially large quantities of *w*MelCS
330 throughout the whole oocyte and at the posterior (Figure S7), as compared to all the other
331 oocytes we examined (e.g., Figure S3). *w*MelCS is only found at low frequencies in a few
332 populations of *D. melanogaster*[75,85], which is attributed to the fact that ancestral *w*MelCS was
333 largely replaced by *w*Mel in global populations of *D. melanogaster* in roughly the last 50 to 100
334 years[86–89]. Perhaps deleterious host effects associated with a high cellular *w*MelCS abundance in
335 oocytes may have contributed to the global replacement of *w*MelCS by *w*Mel. To ensure
336 maternal transmission, *Wolbachia* cells must maintain an association with the host germline
337 without perturbing highly conserved processes of germline and oocyte development[15,62,63,73].
338 Migration of *w*Mel to the posterior germ plasm is coincident with recruitment of host factors
339 required from germline formation and anterior/posterior and dorsal/ventral axis formation[62] and
340 an excessively high *Wolbachia* abundance can disrupt dorsal/ventral axis determination[60,62,73,90].
341 Perhaps similar deleterious effects may help explain why the highly abundant *w*MelCS strain
342 was replaced by *w*Mel, despite a higher rate of transmission in the cold. Previous works has
343 shown that higher densities of *w*MelCS in *D. melanogaster* often covaries with a reduced
344 lifespan[75]. The cellular abundance and fitness consequences of *w*MelCS (as compared to *w*Mel)
345 may also be influenced by interactions with the host genome and the environment[20,21,91]. Indeed,
346 our phylogenetic analyses suggest that the host genome contributes to *Wolbachia* abundance in
347 oocytes (Table S6). Given that interactions with *Wolbachia* and the environment influence host
348 fitness (e.g., fecundity and longevity), it is difficult to point to a single explanation for why
349 *w*MelCS was globally replaced by *w*Mel.
350 The divergent B-group *w*Mau strain was the only strain where transmission significantly
351 increased at 20°C (Figure 2). Transmission was high at 25°C and increased to perfect at 20°C.
352 Our previous work suggests the *w*Mau strain may also be an outlier in its mode of transmission
353 during oogenesis relative to A-group *Wolbachia*, which tend to exhibit evidence of a germline-
354 to-germline route of transmission[15]. *w*Mau occurs at relatively low abundance at the posterior
355 cortex of stage 10 oocytes (Figure 4), but *w*Mau cells are frequently found within the somatically
356 derived follicle cells surrounding the oocytes (Figure S7)[15], which is consistent with a soma-to-
357 germline route of transmission. The presence of *Wolbachia* in the follicle cells is generally not
358 the case for A-group *Wolbachia* (with the exception of *w*Mel, discussed above). We found that
359 *w*Mau was also one of the few strains (in addition to *w*Cha) where *Wolbachia* density in the

360 somatic carcass tissues significantly increased at 20°C (Figure 3), which may help explain why
361 transmission increased slightly at 20°C. *w*Mau transmission was also strongly correlated with
362 *Wolbachia* densities in the carcasses of individual females. Notably, our previous analysis of two
363 other *w*Mau-*D. mauritiana* genotypes using three- to five-day old females found perfect rates of
364 transmission at 25°C[40], unlike our results here (Figure 2). This suggests that differences in fly
365 age[81], the *Wolbachia* and host genomes[21], or other unknown factors may also contribute to
366 variation in rates of maternal transmission.

367 The *w*Mau findings also may inform our previous work on the thermoregulatory behavior
368 of *Drosophila* host species. We found that *Drosophila* species carrying A-group *Wolbachia*,
369 including *w*Ri and *w*Ha, tend to prefer cooler temperatures on a thermogradient (relative to flies
370 without *Wolbachia*), whereas *D. mauritiana* flies carrying *w*Mau prefer warmer temperatures[66].
371 Taken together, these results suggest that fly movement to cool temperatures reduces the density
372 of A-group *Wolbachia* in host tissues, whereas movement to warm temperatures reduces B-
373 group *w*Mau density. This is consistent with the inference that flies may thermoregulate as a
374 behavioral response to ameliorate negative effects of infection and a high *Wolbachia* density[67,92–
375 95]. Movement to cooler temperatures with A-group *Wolbachia* (i.e., behavioral chill) and to
376 warmer temperatures with B-group *w*Mau (behavioral fever) are both behaviors that would
377 reduce *Wolbachia* density in host tissues according to our results here (Figure 3). This finding
378 motives further work dissecting the relationships among thermoregulatory behavior, *Wolbachia*
379 density in host tissues, and maternal transmission.

380 Our phylogenomic analyses revealed that *Wolbachia* density in the ovaries at 25°C and
381 cellular *Wolbachia* abundance in the oocyte posterior region and cortex at 20°C all exhibit
382 phylogenetic signal on the host phylogeny (Table S6, Figure S5), implying that factors in the
383 host genome help explain the observed diversity in *Wolbachia* localization across species. For
384 example, interspecific variation in the host proteins that *Wolbachia* engage during oogenesis
385 could plausibly influence *Wolbachia* localization patterns at the posterior cortex in stage 10
386 oocytes[15]. Unfortunately, it is not yet known how *Wolbachia* engage host factors like kinesin
387 during oogenesis[63]. Other work also suggests the host genome can influence *Wolbachia*
388 abundance in oocytes[21] and embryos[60]. Similarly, genome-wide screens reveal that host factors
389 play an important role in determining cellular *Wolbachia* abundance[96,97]. The findings here
390 complement our previous comparative analyses that suggest the *Wolbachia* genome also

391 contributes to variation in *Wolbachia* localization patterns in oocytes[15] and effects on host
392 thermoregulatory behavior[66]. While we did not identify any traits that exhibit phylogenetic signal
393 on the *Wolbachia* phylogeny, it is worth noting that relatively few *Wolbachia* genomic changes
394 (e.g., in the ampliconic "Octomom" gene region) are required to influence density and tissue
395 distributions[75,98–101]. This highlights the potential for rapid changes in these traits and their
396 effects on transmission. DNA analyses reveal discordant *Wolbachia* and host phylogenies, with
397 recently diverged *Wolbachia* found in distantly related hosts[47–54,102]. This includes evidence of
398 the rapid spread of *w*Ri-like *Wolbachia* across *Drosophila* flies diverged about 50 MYA[51] and
399 *w*Mel-like *Wolbachia* across holometabolous insects[103] diverged about 350 MYA[53]. Given the
400 short persistence of *Wolbachia* with hosts in our study (see Figure S8), it is unlikely that the
401 observed patterns of *Wolbachia* transmission and tissue localization result from coevolution
402 between *Wolbachia* and host genomes.
403 The rate of *Wolbachia* maternal transmission, in conjunction with *Wolbachia* effects on
404 host fitness and cytoplasmic compatibility (CI), ultimately determine *Wolbachia* prevalence in
405 host populations[17,55]. In this study, we uncovered limited variation in maternal transmission rates
406 across temperatures, despite dramatic variation in *Wolbachia* localization patterns within host
407 tissues. Nonetheless, a few *Wolbachia* strains, particularly *w*Mel, had variable transmission rates
408 that are likely to impact *Wolbachia* prevalence in natural host populations. For instance *w*Mel
409 tends to cause weak CI[81,104,105] and occurs at lower frequencies in temperate host populations in
410 Australia and North America, which can plausibly be explained by declining maternal
411 transmission at cool temperatures (Figure 2)[21]. Similarly, *w*Mau does not cause CI and occurs at
412 intermediate frequencies in *D. mauritiana* on Mauritius[40,106]. Our results suggest temperature-
413 related variation in *w*Mau transmission may perhaps help contribute to intermediate frequencies.
414 Supporting our prior observations[20,21], *Wolbachia* transmission rates to female offspring were
415 lower than to male offspring (Table S2), which could influence sex-specific *Wolbachia*
416 frequencies observed in nature. Future work focused on understanding the causes of sex-specific
417 transmission rates and *Wolbachia* densities will be important for understanding this pattern.
418 Other *Wolbachia* strains like *w*Ri[17–19,107], *w*Ha[108–110], and *w*Ana[111,112] cause strong CI and
419 tend to occur at high equilibrium frequencies in nature. In addition to strong CI, our results
420 suggest that stable transmission rates may help these strains maintain high frequencies in the face
421 of fluctuating conditions (Figure 2). However, this may not always be the case, as we found that

422 maternal transmission the strong CI-causing strain *w*Aura[51,111] can be perturbed by temperature.
423 Unlike CI and *Wolbachia* maternal transmission, the role of *Wolbachia* effects on host fitness in
424 natural *Drosophila* populations is poorly understood, although recent work suggests *Wolbachia*
425 block viruses in their native *Drosophila* hosts[8,9,113,114].
426 Understanding how temperature influences *Wolbachia* maternal transmission, especially
427 in relation to other key factors like CI and host fitness effects, is critical for explaining global
428 *Wolbachia* prevalence in host populations. Research on this front will also inform *Wolbachia*-
429 based biocontrol programs, as thermally stable *Wolbachia* strains can be leveraged to improve
430 the efficacy of *Wolbachia*-based biocontrol applications in mosquito populations that experience
431 extreme environments[25,115]. In this respect, temperature and the environment are emerging as key
432 factors that mediate interactions between *Wolbachia*, their hosts, and pathogens.
433
434 **METHODS**
435 *Fly lines*
436 We evaluated 10 different *Wolbachia* strains that naturally occur in eight different
437 *Drosophila* species (Table S1). For two of these host species, we tested multiple *Wolbachia*-host
438 genotypes: *w*Mel and *w*MelCS in *D. melanogaster* and *w*Ri and *w*Ha in *D. simulans*. With the
439 exception of the *w*MelCS-*D. melanogaster* line, all the *Wolbachia*-host genotypes were sampled
440 from nature to form isofemale lines, such that single gravid females were collected from the field
441 and placed individually into vials (see Hague et al., 2020[66] for further discussion of the *w*MelCS
442 genotype). Each isofemale line was stably maintained in the lab for at least four years prior to the
443 experiments. For the maternal transmission experiments explained below, we paired each
444 *Wolbachia*-positive female with *Wolbachia*-free males of the same host species (Table S1). Here,
445 we used males from naturally *Wolbachia*-free isofemale lines whenever possible; however, in
446 some cases, we were unable to obtain natural genotypes without *Wolbachia*. For these species,
447 *Wolbachia*-free genotypes were created by treating the *Wolbachia*-positive genotype with 0.03%
448 tetracycline for at least four generations. After the fourth generation, we used quantitative PCR
449 (qPCR) to confirm that flies were cleared of *Wolbachia*[66]. We then reconstituted the gut
450 microbiome of the tetracycline-cleared flies by rearing them on food where *Wolbachia*-positive
451 males of the same genotype had been fed and defecated for the prior 48 hours. Tetracycline-

452 cleared flies were given at least three more generations before we conducted experiments to
453 avoid detrimental effect of the antibiotic treatment on mitochondrial function[116].
454
455 *Maternal transmission*
456 We tested how temperature influences maternal transmission and *Wolbachia* distributions
457 in host tissues by rearing females of each genotype at a moderate (25°C) and low (20°C)
458 temperatures. Prior to experiments, the isofemale lines were reared for at least two generations in
459 incubators set to each temperature and a 12L:12D light cycle (Percival Model I-36LL) on a
460 standard food diet[66]. We estimated maternal transmission at each temperature by aspirating
461 individual virgin females into vials with two 3-5 day old virgin males of the *Wolbachia*-free
462 genotype and then allowing females to lay eggs for eight days[20,21]. We crossed *Wolbachia*-
463 positive females to males without *Wolbachia*, because in crosses with *Wolbachia*-positive males,
464 *Wolbachia*-free ova produced by *Wolbachia*-positive females could be lost if they are susceptible
465 to cytoplasmic incompatibility, potentially leading to an overestimation of maternal
466 transmission[18]. The males in our experiments were all collected from the *Wolbachia*-free
467 genotypes that were maintained at 25°C.
468 Newly emerged adult F1 offspring were collected in the first 48 hours of emergence,
469 preserved in 95% ethanol, and stored at -20°C for later analysis of *Wolbachia* status. For each
470 subline, we measured maternal transmission by screening five female and five male F1s for
471 *Wolbachia* using PCR. We extracted DNA from individual F1s using 96-well plates and a
472 "squish" extraction buffer (10 mL Tris-HCl [1M], 0.0372 g EDTA, 0.1461 g NaCl, 90 mL dH20,
473 followed by 150 mL Proteinase K after autoclaving) that allows for high-throughput and cost-
474 effective DNA extraction. We screened each F1 for *Wolbachia* status using previously described
475 PCR primers for the *Wolbachia* surface protein (*wsp*) and a second set of primers for the
476 arthropod-specific 28S rDNA that served as a positive control[20,40,117].
477 We computed maternal transmission for each genotype at each temperature as the mean
478 proportion of *Wolbachia*-positive offspring produced by *Wolbachia*-positive mothers in each
479 subline. We then estimated 95% bias-corrected and accelerated bootstrap (BC_a) confidence
480 intervals using the "boot.ci" function and 5000 iterations in the *boot* package in R[118,119]. We
481 analyzed whether maternal transmission rates vary by *Wolbachia*-host genotype (e.g., *w*Mel-*D.*
482 *melanogaster*) and temperature using a generalized linear mixed model (GLMM) logistic

483 regression with the "glmer" function in the *lme4* R package[120]. We treated the *Wolbachia* status
484 of F1s as the dependent variable and then included sex, the *Wolbachia*-host genotype,
485 temperature, and a two-way interaction between the *Wolbachia*-host genotype and temperature
486 as independent variables. We included sex in the model because we previously found that *w*Mel-
487 like *Wolbachia* (*w*Mel and *w*Yak) are transmitted more efficiently to male offspring[20,21]. Finally,
488 we included the subline of each F1 as a random effect. We assessed significance of the fixed
489 effects with a likelihood ratio test (LRT) and type III sum of squares using the "mixed" function
490 in the *afex* package[121]. Lastly, we used two-sided Wilcoxon rank-sum tests to evaluate whether
491 transmission rates differ between 25° and 20°C for each strain.
492
493 *Wolbachia density in host ovaries*
494 After each female was allowed to lay for eight days, we immediately dissected out her
495 ovaries in chilled 1X PBS. Both the ovaries and remaining carcass were then frozen at -80°C.
496 We then used qPCR to quantify *Wolbachia* density in the dissected ovaries and carcasses of each
497 individual female. DNA was first extracted using a DNeasy Blood and Tissue Kit (Qiagen) and
498 then amplified the *Wolbachia*-specific locus *ftsZ* and the *Drosophila*-specific locus *nAcRalpha-*
499 *34E*. Preliminary analyses indicated that separate primers were needed for *Wolbachia* in the
500 divergent A-Group (F: 5'-ATCCTTAACTGCGGCTCTTG-3', R: 5'-
501 TTCATCACAGCAGGAATGGG-3') and B-Group lineages (F: 5'-
502 CAGAGAAGCAAGAGCGGTAG-3', R: 5'-TCTTCAAGTCCAAGCTCTGC -3'). We were
503 able to use a single set of primers for all the *Drosophila* hosts (F: 5'-
504 CTATGGTCGTTGACAGACT-3', R: 5'-GTAGTACAGCTATTG TGGC-3'). We generated
505 efficiency curves to confirm that each primer pair amplified with adequate efficiency for each
506 *Wolbachia* strain and host species. The individual 10 µl reactions included 5 µl PowerUp SYBR
507 Green Master Mix (Applied Biosystems), 0.25 µl of the forward and reverse primers, 0.5 µl of
508 water, and 4 µl of gDNA. All qPCR reactions were amplified using the following cycling
509 conditions: 50°C for 2 min, 95°C for 2 min, and then 40 cycles, with one cycle consisting of
510 95°C for 15 s, 58°C for 15 s, and 72°C for 1 min. We used the average cycle threshold (Ct) value
511 of three technical replicates for each sample. We then estimated relative *Wolbachia* density as
512 $2^{\Delta Ct}$, where $\Delta Ct = Ct_{nAcRalpha-34E} - Ct_{ftsZ}$[122]. We used a two-way ANOVA and type III
513 sums of squares to test whether log-transformed *Wolbachia* density varied among *Wolbachia*-

514 host genotypes and temperature for both the ovaries and the carcasses. We also used two-sided
515 Wilcoxon rank-sum tests to test whether densities differed between 25° and 20°C for each tissue
516 and *Wolbachia*-host genotype. If endoreplication in nurse cells is altered by temperature, changes
517 to host ploidy in ovary tissues could plausibly influence our estimates of relative *Wolbachia*
518 density ($2^{\Delta Ct}$) at each temperature[72]. We evaluated the raw Ct values for evidence of temperature
519 differences in copy number at the host locus *nAcRalpha-34E* (Figure S6) and found that host
520 ovary Ct values did not change significantly between temperature treatments, implying that
521 differences in relative *Wolbachia* density are due to changes in absolute abundance of the
522 *Wolbachia* gene.
523
524 *Cellular Wolbachia abundance in host oocytes*
525 We used previously described protocols and confocal imaging to quantify cellular
526 *Wolbachia* in host oocytes at each temperature[15,21]. Briefly, we paired 20 newly emerged virgin
527 *Wolbachia*-positive females *en masse* with ten 3-5 day old virgin *Wolbachia*-negative males in
528 individual vials for eight days to stimulate oocyte production. Females were then separated using
529 CO_2 and ovaries were dissected in a chilled dish of 1X PBS. Ovaries were fixed in 200 µl of
530 devitellinizing solution (2% paraformaldehyde and 0.5% v/v NP40 in 1X PBS) mixed with 600
531 µl of heptane for 20 min on a shaker at room temperature. We then removed the organic layer
532 using a brief centrifugation and washed the ovaries three times with PBS-T (0.1% Triton X-100
533 in 1X PBS), followed by three additional five min washes. Samples were treated with RNAse A
534 (10 mg/ml) and left overnight at room temperature. The samples were then washed in PBS-T
535 multiple times over two hours and then stained with a dilute solution of Alexa 488 phalloidin on
536 a shaker for two hours for actin staining. Subsequently, the samples were washed again multiple
537 times over the course of two more hour. Finally, the wash solution was removed and we added
538 60 µl of propidium iodide (PI) in mounting media (VECTASHIELD) and left again overnight.
539 Ovaries were then mounted and carefully separated out again for ease of imaging. Slides were
540 sealed with a coat of nail polish and stored at -20°C until imaging.
541 We used a Zeiss Olympia confocal microscope and the 40x Plan-Apochromat oil
542 objective for image acquisition. Alexa 488 was imaged using the 488 nm laser line and emissions
543 were collected from 493 to 584 nm. Propidium iodide was imaged using the 488 and 561 nm
544 lines and emissions were collected from 584 to 718 nm. Stage 10 oocytes were identified based

545 on two criterion. First, the egg chamber had to have two compartments, one with nurse cells and
546 the other with the developing oocyte. Second, the oocyte had to account for approximately 50%
547 of the egg chamber. The top and bottom of the oocyte were identified by scanning through the
548 egg chamber and then a 0.8 μm slice was taken around the midplane. The pixel dwell time was
549 8.19 μsec.

550 Image analysis was conducted in the program Fiji[123] following Russell *et al.*[63]. We first
551 manually adjusted the contrast of each image to increase the threshold so that only white puncta
552 corresponding to *Wolbachia* cells inside the oocyte were retained and all background noise was
553 rendered black. We then used the polygon selection tool to select three different regions of the
554 oocyte (see Figure S1 in Russell *et al.*): the whole oocyte, the posterior region, and the posterior
555 cortex. We defined the posterior region as the posterior 1/8th of the oocyte and the posterior
556 cortex as the narrow cortical region where the pole plasm component Vasa is expressed[15,63]. The
557 "area" and "integrated density" were measured for each region. Additionally, the average of a
558 quadruplicate measure of "mean gray value" in background selections was measured to account
559 for any remaining background fluorescence. The corrected total cell fluorescence (CTCF) was
560 calculated as integrated density – (area x background mean gray value) for each region. We used
561 two-way ANOVAs and type III sums of squares to test whether log-transformed CTCF values
562 differed among *Wolbachia*-host genotypes and temperature in each region of the oocyte (whole
563 oocyte, posterior region, and posterior cortex). We also used two-sided Wilcoxon rank-sum tests
564 to test whether CTCF values differed between 25° and 20°C for each oocyte regions and
565 *Wolbachia*-host genotype.
566
567 *Phylogenomic analyses*

568 We conducted phylogenomic analyses to characterize the evolutionary relationships
569 among *Wolbachia* strains and *Drosophila* host species. We obtained *Wolbachia* sequences from
570 publicly available genome assemblies for *w*Mel[21], *w*MelCS[66], *w*Seg, *w*Cha[15], *w*Ri[124], *w*Ana[125],
571 *w*Aura, *w*Tri[51], *w*Ha[126], and *w*Mau[40]. We used Prokka 1.11 to identify homologs to known
572 bacterial genes in the assemblies[127]. We avoided pseudogenes and paralogs in our phylogenetic
573 analyses by selecting only single copy genes that uniquely matched a bacterial reference gene
574 identified by Prokka. We removed loci with indels by requiring all homologs to have identical
575 length in all *Wolbachia* genomes. A total of 170 full length single copy genes met these criteria,

576 totaling 135,105 bp. We then estimated a Bayesian phylogram using RevBayes 1.0.8 under the
577 GTR + Γ + I model partitioned by codon position[128]. Four independent runs were performed,
578 which all converged on the same topology. All nodes were supported with Bayesian posterior
579 probabilities >0.99.

580 To estimate an absolute chronogram for *Wolbachia*, we first estimated a relaxed-clock
581 relative chronogram using RevBayes[128] with the root age fixed to 1 using the GTR + Γ + I,
582 partitioned by codon position, using the same birth-death prior as Turelli et al (2018)[51]. Each
583 partition had an independent rate multiplier with prior Γ(1,1), as well as stationary frequencies
584 and exchangeability rates drawn from flat, symmetrical Dirichlet distributions. For each branch,
585 the branch-rate prior was Γ(7,7), normalized to a mean of 1 across all branches. We performed
586 four independent runs that all agreed. We converted the relative chronogram into an absolute
587 chronogram using the scaled distribution $\Gamma(7,7) \times 6.87 \times 10^{-9}$ substitutions per third position site
588 per year, derived from the posterior distribution estimated by Richardson et al. (2012)[85],
589 assuming 10 generations per year. Absolute branch lengths were calculated as the relative branch
590 length times the third position rate multiplier divided by the substitutions per third-position site
591 per year estimate above.

592 We used similar methods to generate a phylogram for the *Drosophila* host species.
593 Publicly available sequences were obtained for *D. melanogaster*[129], *D. simulans*[130], *D.*
594 *mauritiana*[40], *D. seguyi*, *D. chauvacae*[131], *D. auraria*, *D. triauraria*[51], and *D. ananassae*[132]. A
595 host phylogeny was generated using the same nuclear genes implemented in Turelli *et al.*[51]:
596 *aconitase, aldolase, bicoid, ebony, enolase, esc, g6pdh, glyp, glys, ninaE, pepck, pgi, pgm, pic,*
597 *ptc, tpi, transaldolase, white, wingless,* and *yellow*. We used BLAST with the *D. melanogaster*
598 coding sequences to extract orthologs from the genomes of each host species. Sequences were
599 then aligned with MAFFT 7[133]. Finally, we used RevBayes and the GTR + Γ + I model
600 partitioned by codon position and gene to accommodate potential variation in the substitution
601 process among genes. All nodes were supported with Bayesian posterior probabilities of 1.

602 The resulting phylograms were used to test whether *Wolbachia* density and oocyte
603 cellular abundance exhibit phylogenetic signal on either the *Wolbachia* or host phylogenies. For
604 the host phylogeny, we pooled estimates of *Wolbachia* density and oocyte abundance by host
605 species, because two of the hosts (*D. melanogaster* and *D. simulans*) had data for multiple
606 genotypes carrying different *Wolbachia* strains. We used our estimates of *Wolbachia* density

607 ($2^{\Delta Ct}$) and cellular oocyte abundance (log-transformed CTCF) to test for phylogenetic signal
608 using Pagel's lambda (λ)[68]. A Pagel's λ of 0 indicates that character evolution occurs
609 independently of phylogenetic relationships, whereas λ = 1 is consistent with a Brownian motion
610 model of character evolution. We used the "phylosig" function and a likelihood ratio test (LRT)
611 in the *phytools* package[134] to compare the fitted value to a model assuming no phylogenetic
612 signal (λ = 0). We also used a Monte Carlo-based method to generate 95% confidence intervals
613 surrounding our estimates using 1,000 bootstrap replicates in the *pmc* package[135].
614
615 *Statistics and reproducibility*
616 All statistical analyses were performed in R[119]. Specific details for each statistical
617 analysis are reported above. We conducted distribution and leverage analyses to evaluate
618 assumptions of normality and then used data transformations and non-parametric tests when
619 applicable (described above). Samples sizes and test statistics for each *Wolbachia*-host genotype
620 are reported in the Supplementary Information. For each experiment, we collected the largest
621 sample size that was feasible within our experimental design. We do not report any issues with
622 reproducibility.
623
624 **ACKNOWLEDGEMENTS**
625 We are especially thankful to W. Sullivan for very useful discussions that improved the
626 quality of this manuscript. We thank W. Conner for assistance with bioinformatic analyses. J.
627 Statz provided thoughtful feedback on the manuscript. Support and instrumentation was provided
628 by the Cellular Genetics Ecosystem in the Genomics Core, the Environmental Control for
629 Organismal Research (ECOR) facility, and the Center for Biomolecular Structure and Dynamics
630 at the University of Montana. This study was funded by a National Science Foundation
631 CAREER (2145195) Award to BSC. BSC was also supported by a National Institute of General
632 Medical Sciences of the National Institutes of Health MIRA Award (R35GM124701).
633
634 **AUTHOR CONTRIBUTIONS**
635 M.T.J.H. designed the project, collected data, performed analyses, and prepared the
636 manuscript. T.B.W. collected data. B.S.C. acquired funding, designed the project, prepared the

637 manuscript, and provided leadership. All authors reviewed and edited the manuscript prior to
638 submission.
639
640 **COMEPETING INTERESTS**
641 The authors declare no competing interests.
642
643 **DATA AVAILABILITY**
644 All source data on the estimation of maternal transmission, *Wolbachia* densities, and
645 cellular *Wolbachia* abundance are included as Supplementary Data files.
646
647 **FIGURES**
648 **Figure 1. Divergent *Wolbachia* strains found in *Drosophila* host species. (a)** Estimated
649 Bayesian phylogram of the 10 A- and B-group *Wolbachia* strains included in the study. The
650 phylogram was estimated using 170 single-copy genes of identical length in all genomes,
651 spanning 135,105 bp. **(b)** Estimated Bayesian phylogram of the eight *Drosophila* species using
652 20 single-copy genes. All nodes on both trees are supported with Bayesian posterior probabilities
653 of 1. Estimates of *Wolbachia* and *Drosophila* divergence reported in millions of years ago
654 (MYA) are reproduced from Meany *et al.*[40] and Suvorov *et al.*[136], respectively. The *Wolbachia*
655 and host trees are generally discordant, as expected with frequent *Wolbachia* host
656 switching[47,48,51,53,54].
657
658 **Figure 2. Maternal transmission is high and stable across temperatures for many**
659 ***Wolbachia* strains.** Mean maternal transmission rates (±BC_a confidence intervals) of different
660 *Wolbachia* strains in their naturally associated host species (N = 364 sublines). Asterisks indicate
661 the rates of maternal transmission differ between 25° and 20°C for a given *Wolbachia* strain
662 according to a Wilcoxon rank-sum test at $P < 0.05$. Below, the cladogram depicts evolutionary
663 relationships among *Wolbachia* strains.
664
665 **Figure 3. *Wolbachia* densities in host tissues vary by *Wolbachia*-host system and**
666 **temperature.** *Wolbachia* densities are shown for dissected female ovaries and the remaining
667 somatic carcass tissue (N = 183 F0 females). Asterisks indicate the *Wolbachia* density differs

668 between 25° and 20°C for a given *Wolbachia* strain according to a Wilcoxon rank-sum test at P
669 < 0.05. Boxplots show medians, first and third quartiles (hinges), and the smallest/largest values
670 within 1.5*IQR of the hinges (whiskers).
671
672 **Figure 4. Cellular *Wolbachia* abundance in late-stage oocytes generally does not align with**
673 **maternal transmission rates.** Cellular *Wolbachia* abundance in stage 10 oocytes (measured as
674 fluorescence due to propidium iodide; CTCF), measured in **(a)** the whole oocyte, **(b)** the
675 posterior region, and **(c)** the posterior cortex ($N = 283$ oocytes). Asterisks indicate that
676 *Wolbachia* abundance differs between 25° and 20°C for a given *Wolbachia* strain according to a
677 Wilcoxon rank-sum test at $P < 0.05$. **(d)** Representative confocal images of *Wolbachia* strains
678 that have decreased abundance at the posterior cortex in the cold (*w*Mel), increased abundance at
679 the cortex in the cold (*w*Ri), and no change in the cold (*w*Cha). Confocal micrographs are DNA-
680 stained with PI (red) and actin-stained with phalloidin (green). The second column depicts a
681 single channel image of the PI stain and the third column depicts an enlarged PI-stained image at
682 the posterior cortex of each oocyte. Scale bars are set to 25 µm.
683
684 **REFERENCES**

685 1. Sudakaran, S., Kost, C. & Kaltenpoth, M. Symbiont acquisition and replacement as a
686 source of ecological innovation. *Trends Microbiol.* **25**, 375–390 (2017).
687 2. McCutcheon, J. P., Boyd, B. M. & Dale, C. The life of an insect endosymbiont from the
688 cradle to the grave. *Curr. Biol.* **29**, R485–R495 (2019).
689 3. McCutcheon, J. P. The genomics and cell biology of host-beneficial intracellular infections.
690 *Annu. Rev. Cell Dev. Biol.* **37**, 115–142 (2021).
691 4. Werren, J. H., Baldo, L. & Clark, M. E. *Wolbachia:* master manipulators of invertebrate
692 biology. *Nat. Rev. Microbiol.* **6**, 741–751 (2008).
693 5. Shropshire, J. D., Leigh, B. & Bordenstein, S. R. Symbiont-mediated cytoplasmic
694 incompatibility: what have we learned in 50 years? *Elife* **9**, e61989 (2020).
695 6. Oliver, K. M., Russell, J. A., Moran, N. A. & Hunter, M. S. Facultative bacterial symbionts
696 in aphids confer resistance to parasitic wasps. *Proc. Natl. Acad. Sci.* **100**, 1803–1807
697 (2003).
698 7. Jaenike, J., Unckless, R., Cockburn, S. N., Boelio, L. M. & Perlman, S. J. Adaptation via
699 symbiosis: recent spread of a *Drosophila* defensive symbiont. *Science* **329**, 212–215
700 (2010).
701 8. Cogni, R., Ding, S. D., Pimentel, A. C., Day, J. P. & Jiggins, F. M. *Wolbachia* reduces virus
702 infection in a natural population of *Drosophila*. *Commun. Biol.* **4**, 1–7 (2021).

703 9. Bruner-Montero, G. & Jiggins, F. M. *Wolbachia* protects *Drosophila melanogaster* against
704 two naturally occurring and virulent viral pathogens. *Sci. Rep.* **13**, 8518 (2023).

705 10. Baumann, P. Biology of bacteriocyte-associated endosymbionts of plant sap-sucking
706 insects. *Annu. Rev. Microbiol.* **59**, 155–189 (2005).

707 11. Moran, N. A., McCutcheon, J. P. & Nakabachi, A. Genomics and evolution of heritable
708 bacterial symbionts. *Annu. Rev. Genet.* **42**, 165–190 (2008).

709 12. Douglas, A. E. The microbial dimension in insect nutritional ecology. *Funct. Ecol.* **23**, 38–
710 47 (2009).

711 13. Fisher, R. M., Henry, L. M., Cornwallis, C. K., Kiers, E. T. & West, S. A. The evolution of
712 host-symbiont dependence. *Nat. Commun.* **8**, 1–8 (2017).

713 14. Russell, S. L., Chappell, L. & Sullivan, W. A symbiont's guide to the germline. *Curr. Top.*
714 *Dev. Biol.* **135**, 315–351 (2019).

715 15. Radousky, Y. A. *et al.* Distinct *Wolbachia* localization patterns in oocytes of diverse host
716 species reveal multiple strategies of maternal transmission. *Genetics* **224**, (2023).

717 16. Dunbar, H. E., Wilson, A. C., Ferguson, N. R. & Moran, N. A. Aphid thermal tolerance is
718 governed by a point mutation in bacterial symbionts. *PLoS Biol.* **5**, (2007).

719 17. Hoffmann, A. A., Turelli, M. & Harshman, L. G. Factors affecting the distribution of
720 cytoplasmic incompatibility in *Drosophila simulans*. *Genetics* **126**, 933–948 (1990).

721 18. Turelli, M. & Hoffmann, A. A. Cytoplasmic incompatibility in *Drosophila simulans*:
722 dynamics and parameter estimates from natural populations. *Genetics* **140**, 1319–1338
723 (1995).

724 19. Carrington, L. B., Lipkowitz, J. R., Hoffmann, A. A. & Turelli, M. A re-examination of
725 *Wolbachia*-induced cytoplasmic incompatibility in California *Drosophila simulans*. *PLoS*
726 *One* **6**, e22565 (2011).

727 20. Hague, M. T., Mavengere, H., Matute, D. R. & Cooper, B. S. Environmental and genetic
728 contributions to imperfect *w*Mel-like *Wolbachia* transmission and frequency variation.
729 *Genetics* **215**, 1117–1132 (2020).

730 21. Hague, M. T. J. *et al.* Temperature effects on cellular host-microbe interactions explain
731 continent-wide endosymbiont prevalence. *Curr. Biol.* **32**, 878-888.e8 (2022).

732 22. Wade, M. J. The co-evolutionary genetics of ecological communities. *Nat. Rev. Genet.* **8**,
733 185–195 (2007).

734 23. Weeks, A. R., Turelli, M., Harcombe, W. R., Reynolds, K. T. & Hoffmann, A. A. From
735 parasite to mutualist: Rapid evolution of *Wolbachia* in natural populations of *Drosophila*.
736 *PLoS Biol.* **5**, e114 (2007).

737 24. Ross, P. A., Turelli, M. & Hoffmann, A. A. Evolutionary ecology of *Wolbachia* releases for
738 disease control. *Annu. Rev. Genet.* **53**, (2019).

739 25. Ross, P. A. *et al.* Developing *Wolbachia*-based disease interventions for an extreme
740 environment. *PLoS Pathog.* **19**, e1011117 (2023).

741 26. Hien, N. T. *et al.* Environmental factors influence the local establishment of *Wolbachia* in
742 *Aedes aegypti* mosquitoes in two small communities in central Vietnam. *Gates Open Res.* **5**,
743 (2021).

744 27. Nikolouli, K. *et al.* Sterile insect technique and *Wolbachia* symbiosis as potential tools for
745 the control of the invasive species *Drosophila suzukii*. *J. Pest Sci.* **91**, 489–503 (2018).

746 28. Gong, J.-T. *et al.* Stable introduction of plant-virus-inhibiting *Wolbachia* into planthoppers
747 for rice protection. *Curr. Biol.* **30**, 4837–4845 (2020).

748 29. McMeniman, C. J. *et al.* Stable introduction of a life-shortening *Wolbachia* infection into
749 the mosquito *Aedes aegypti*. *Science* **323**, 141–144 (2009).

750 30. Hoffmann, A. A. *et al.* Successful establishment of *Wolbachia* in *Aedes* populations to
751 suppress dengue transmission. *Nature* **476**, 454–457 (2011).

752 31. Walker, T. *et al.* The *w*Mel *Wolbachia* strain blocks dengue and invades caged *Aedes*
753 *aegypti* populations. *Nature* **476**, 450–453 (2011).

754 32. Utarini, A. *et al.* Efficacy of *Wolbachia*-infected mosquito deployments for the control of
755 dengue. *N. Engl. J. Med.* **384**, 2177–2186 (2021).

756 33. Ross, P. A. *et al. Wolbachia* infections in *Aedes aegypti* differ markedly in their response to
757 cyclical heat stress. *PLOS Pathog.* **13**, e1006006 (2017).

758 34. Ross, P. A., Ritchie, S. A., Axford, J. K. & Hoffmann, A. A. Loss of cytoplasmic
759 incompatibility in *Wolbachia*-infected *Aedes aegypti* under field conditions. *PLoS Negl.*
760 *Trop. Dis.* **13**, e0007357 (2019).

761 35. Funkhouser-Jones, L. J., van Opstal, E. J., Sharma, A. & Bordenstein, S. R. The maternal
762 effect gene Wds controls *Wolbachia* titer in *Nasonia*. *Curr. Biol.* **28**, 1692–1702 (2018).

763 36. Porter, J. & Sullivan, W. The cellular lives of *Wolbachia*. *Nat. Rev. Microbiol.* 1–17 (2023).

764 37. Bright, M. & Bulgheresi, S. A complex journey: transmission of microbial symbionts. *Nat.*
765 *Rev. Microbiol.* **8**, 218–230 (2010).

766 38. Landmann, F. *et al.* Both asymmetric mitotic segregation and cell-to-cell invasion are
767 required for stable germline transmission of *Wolbachia* in filarial nematodes. *Biol. Open* **1**,
768 536–547 (2012).

769 39. Correa, C. C. & Ballard, J. *Wolbachia* associations with insects: winning or losing against a
770 master manipulator. *Front. Ecol. Evol.* **3**, 153 (2016).

771 40. Meany, M. K. *et al.* Loss of cytoplasmic incompatibility and minimal fecundity effects
772 explain relatively low *Wolbachia* frequencies in *Drosophila mauritiana*. *Evolution* **73**,
773 1278–1295 (2019).

774 41. Olsen, K., Reynolds, K. T. & Hoffmann, A. A. A field cage test of the effects of the
775 endosymbiont *Wolbachia* on *Drosophila melanogaster*. *Heredity* **86**, 731–737 (2001).

776 42. Hamm, C. A. *et al. Wolbachia* do not live by reproductive manipulation alone: Infection
777 polymorphism in *Drosophila suzukii* and *D. subpulchrella*. *Mol. Ecol.* **23**, 4871–4885
778 (2014).

43. Ross, P. A. *et al.* Heatwaves cause fluctuations in *w*Mel *Wolbachia* densities and frequencies in *Aedes aegypti*. *PLoS Negl. Trop. Dis.* **14**, e0007958 (2020).

44. Ferri, E. *et al.* New insights into the evolution of *Wolbachia* infections in filarial nematodes inferred from a large range of screened species. *PLoS One* **6**, e20843 (2011).

45. Zug, R. & Hammerstein, P. Still a host of hosts for *Wolbachia*: Analysis of recent data suggests that 40% of terrestrial arthropod species are infected. *PLoS One* **7**, e38544 (2012).

46. Weinert, L. A., Araujo-Jnr, E. V., Ahmed, M. Z. & Welch, J. J. The incidence of bacterial endosymbionts in terrestrial arthropods. *Proc. R. Soc. B Biol. Sci.* **282**, 20150249 (2015).

47. O'Neill, S. L., Giordano, R., Colbert, A. M., Karr, T. L. & Robertson, H. M. 16S rRNA phylogenetic analysis of the bacterial endosymbionts associated with cytoplasmic incompatibility in insects. *Proc. Natl. Acad. Sci.* **89**, 2699–2702 (1992).

48. Raychoudhury, R., Baldo, L., Oliveira, D. C. & Werren, J. H. Modes of acquisition of *Wolbachia*: Horizontal transfer, hybrid introgression, and codivergence in the *Nasonia* species complex. *Evolution* **63**, 165–183 (2009).

49. Conner, W. R. *et al.* Genome comparisons indicate recent transfer of *w*Ri-like *Wolbachia* between sister species *Drosophila suzukii* and *D. subpulchrella*. *Ecol. Evol.* **7**, 9391–9404 (2017).

50. Gerth, M. & Bleidorn, C. Comparative genomics provides a timeframe for *Wolbachia* evolution and exposes a recent biotin synthesis operon transfer. *Nat. Microbiol.* **2**, 16241 (2017).

51. Turelli, M. *et al.* Rapid global spread of *w*Ri-like *Wolbachia* across multiple *Drosophila*. *Curr. Biol.* **28**, 963-971.e8 (2018).

52. Cooper, B. S., Vanderpool, D., Conner, W. R., Matute, D. R. & Turelli, M. *Wolbachia* acquisition by *Drosophila yakuba*-clade hosts and transfer of incompatibility loci between distantly related *Wolbachia*. *Genetics* **212**, 1399–1419 (2019).

53. Shropshire, D. *et al.* Rapid turnover of pathogen-blocking *Wolbachia* and their incompatibility loci. *bioRxiv* 2023–12 (2023).

54. Vancaester, E. & Blaxter, M. Phylogenomic analysis of *Wolbachia* genomes from the Darwin Tree of Life biodiversity genomics project. *PLoS Biol.* **21**, e3001972 (2023).

55. Caspari, E. & Watson, G. On the evolutionary importance of cytoplasmic sterility in mosquitoes. *Evolution* **13**, 568–570 (1959).

56. Turelli, M., Katznelson, A. & Ginsberg, P. S. Why *Wolbachia*-induced cytoplasmic incompatibility is so common. *Proc. Natl. Acad. Sci.* **119**, e2211637119 (2022).

57. Turelli, M. & Hoffmann, A. A. Rapid spread of an inherited incompatibility factor in California *Drosophila*. *Nature* **353**, 440–442 (1991).

58. Kriesner, P., Conner, W. R., Weeks, A. R., Turelli, M. & Hoffmann, A. A. Persistence of a *Wolbachia* infection frequency cline in *Drosophila melanogaster* and the possible role of reproductive dormancy. *Evolution* **70**, 979–997 (2016).

59. Hadfield, S. J. & Axton, J. M. Germ cells colonized by endosymbiotic bacteria. *Nature* **402**, 482 (1999).

819 60. Veneti, Z., Clark, M. E., Karr, T. L., Savakis, C. & Bourtzis, K. Heads or tails: host-parasite
820 interactions in the *Drosophila-Wolbachia* system. *Appl. Environ. Microbiol.* **70**, 5366–5372
821 (2004).

822 61. Ferree, P. M. *et al. Wolbachia* utilizes host microtubules and Dynein for anterior
823 localization in the *Drosophila* oocyte. *PLoS Pathog.* **1**, e14 (2005).

824 62. Serbus, L. R. & Sullivan, W. A cellular basis for *Wolbachia* recruitment to the host
825 germline. *PLoS Pathog.* **3**, e190 (2007).

826 63. Russell, S. L., Lemseffer, N. & Sullivan, W. T. *Wolbachia* and host germline components
827 compete for kinesin-mediated transport to the posterior pole of the *Drosophila* oocyte.
828 *PLoS Pathog.* **14**, e1007216 (2018).

829 64. Prout, T. Some evolutionary possibilities for a microbe that causes incompatibility in its
830 host. *Evolution* **48**, 909–911 (1994).

831 65. Turelli, M. Evolution of incompatibility-inducing microbes and their hosts. *Evolution* **48**,
832 1500–1513 (1994).

833 66. Hague, M. T., Caldwell, C. N. & Cooper, B. S. Pervasive effects of *Wolbachia* on host
834 temperature preference. *mBio* **11**, e01768-20 (2020).

835 67. Hague, M. T. J., Woods, H. A. & Cooper, B. S. Pervasive effects of *Wolbachia* on host
836 activity. *Biol. Lett.* **17**, 20210052 (2021).

837 68. Pagel, M. Inferring the historical patterns of biological evolution. *Nature* **401**, 877–884
838 (1999).

839 69. Freckleton, R. P., Harvey, P. H. & Pagel, M. Phylogenetic analysis and comparative data: a
840 test and review of evidence. *Am. Nat.* **160**, 712–726 (2002).

841 70. Rajpurohit, S. & Schmidt, P. S. Measuring thermal behavior in smaller insects: A case
842 study in *Drosophila melanogaster* demonstrates effects of sex, geographic origin, and
843 rearing temperature on adult behavior. *Fly (Austin)* **10**, 149–161 (2016).

844 71. Funkhouser-Jones, L. J., van Opstal, E. J., Sharma, A. & Bordenstein, S. R. The maternal
845 effect gene Wds controls *Wolbachia* titer in *Nasonia*. *Curr. Biol.* **28**, 1692–1702 (2018).

846 72. Christensen, S. *et al.* Quantitative methods for assessing local and bodywide contributions
847 to *Wolbachia* titer in maternal germline cells of *Drosophila*. *BMC Microbiol.* **19**, 1–17
848 (2019).

849 73. Serbus, L. R. *et al.* A feedback loop between *Wolbachia* and the *Drosophila* gurken mRNP
850 complex influences *Wolbachia* titer. *J. Cell Sci.* **124**, 4299–4308 (2011).

851 74. Clark, M. E., Veneti, Z., Bourtzis, K. & Karr, T. L. *Wolbachia* distribution and cytoplasmic
852 incompatibility during sperm development: the cyst as the basic cellular unit of CI
853 expression. *Mech. Dev.* **120**, 185–198 (2003).

854 75. Chrostek, E. *et al. Wolbachia* variants induce differential protection to viruses in
855 *Drosophila melanogaster*: a phenotypic and phylogenomic analysis. *PLoS Genet.* **9**,
856 e1003896 (2013).

857 76. Noda, H., Koizumi, Y., Zhang, Q. & Deng, K. Infection density of *Wolbachia* and
858 incompatibility level in two planthopper species, *Laodelphax striatellus* and *Sogatella*
859 *furcifera*. *Insect Biochem. Mol. Biol.* **31**, 727–737 (2001).

860 77. Duron, O., Fort, P. & Weill, M. Influence of aging on cytoplasmic incompatibility, sperm
861 modification and *Wolbachia* density in *Culex pipiens* mosquitoes. *Heredity* **98**, 368–374
862 (2007).

863 78. Kaur, R., Martinez, J., Rota-Stabelli, O., Jiggins, F. M. & Miller, W. J. Age, tissue,
864 genotype and virus infection regulate *Wolbachia* levels in *Drosophila*. *Mol. Ecol.* **29**, 2063–
865 2079 (2020).

866 79. Tortosa, P. *et al. Wolbachia* age-sex-specific density in *Aedes albopictus*: a host
867 evolutionary response to cytoplasmic incompatibility? *PLoS One* **5**, e9700 (2010).

868 80. Unckless, R. L., Boelio, L. M., Herren, J. K. & Jaenike, J. Wolbachia as populations within
869 individual insects: causes and consequences of density variation in natural populations.
870 *Proc. R. Soc. B Biol. Sci.* **276**, 2805–2811 (2009).

871 81. Shropshire, J. D., Hamant, E. & Cooper, B. S. Male age and *Wolbachia* dynamics:
872 investigating how fast and why bacterial densities and cytoplasmic incompatibility
873 strengths vary. *mBio* **12**, e02998-21 (2021).

874 82. Layton, E. M., On, J., Perlmutter, J. I., Bordenstein, S. R. & Shropshire, J. D. Paternal
875 grandmother age affects the strength of *Wolbachia*-induced cytoplasmic incompatibility in
876 *Drosophila melanogaster*. *mBio* **10**, 10–1128 (2019).

877 83. Frydman, H. M., Li, J. M., Robson, D. N. & Wieschaus, E. Somatic stem cell niche tropism
878 in *Wolbachia*. *Nature* **441**, 509 (2006).

879 84. White, P. M. *et al.* Mechanisms of horizontal cell-to-cell transfer of *Wolbachia* spp. in
880 *Drosophila melanogaster*. *Appl Env. Microbiol* **83**, e03425-16 (2017).

881 85. Richardson, M. F. *et al.* Population genomics of the *Wolbachia* endosymbiont in
882 *Drosophila melanogaster*. *PLoS Genet.* **8**, e1003129 (2012).

883 86. Riegler, M., Sidhu, M., Miller, W. J. & O'Neill, S. L. Evidence for a global *Wolbachia*
884 replacement in *Drosophila melanogaster*. *Curr. Biol.* **15**, 1428–1433 (2005).

885 87. Ilinsky, Y. Coevolution of *Drosophila melanogaster* mtDNA and *Wolbachia* genotypes.
886 *PLoS One* **8**, e54373 (2013).

887 88. Early, A. M. & Clark, A. G. Monophyly of *Wolbachia pipientis* genomes within *Drosophila*
888 *melanogaster*: Geographic structuring, titre variation and host effects across five
889 populations. *Mol. Ecol.* **22**, 5765–5778 (2013).

890 89. Strunov, A. *et al.* Historic museum samples provide evidence for a recent replacement of
891 *Wolbachia* types in European *Drosophila melanogaster*. *Mol. Biol. Evol.* **40**, msad258
892 (2023).

893 90. Poinsot, D., Bourtzis, K., Markakis, G., Savakis, C. & Merçot, H. Wolbachia transfer from
894 *Drosophila melanogaster* into *D. simulans*: Host effect and cytoplasmic incompatibility
895 relationships. *Genetics* **150**, 227–237 (1998).

896 91. Strunov, A., Lerch, S., Blanckenhorn, W. U., Miller, W. J. & Kapun, M. Complex effects of
897 environment and *Wolbachia* infections on the life history of *Drosophila melanogaster*
898 hosts. *J. Evol. Biol.* **35**, 788–802 (2022).

899 92. Hart, B. L. Biological basis of the behavior of sick animals. *Neurosci. Biobehav. Rev.* **12**,
900 123–137 (1988).

901 93. De Roode, J. C. & Lefèvre, T. Behavioral immunity in insects. *Insects* **3**, 789–820 (2012).

902 94. Curtis, V. A. Infection-avoidance behaviour in humans and other animals. *Trends Immunol.*
903 **35**, 457–464 (2014).

904 95. Fedorka, K. M., Kutch, I. C., Collins, L. & Musto, E. Cold temperature preference in
905 bacterially infected *Drosophila melanogaster* improves survival but is remarkably
906 suboptimal. *J. Insect Physiol.* **93**, 36–41 (2016).

907 96. White, P. M. *et al.* Reliance of *Wolbachia* on high rates of host proteolysis revealed by a
908 genome-wide RNAi screen of *Drosophila* cells. *Genetics* **205**, 1473–1488 (2017).

909 97. Grobler, Y. *et al.* Whole genome screen reveals a novel relationship between *Wolbachia*
910 levels and *Drosophila* host translation. *PLoS Pathog.* **14**, e1007445 (2018).

911 98. Chrostek, E. & Teixeira, L. Mutualism breakdown by amplification of *Wolbachia* genes.
912 *PLoS Biol.* **13**, e1002065 (2015).

913 99. Chrostek, E. & Teixeira, L. Within host selection for faster replicating bacterial symbionts.
914 *PLoS One* **13**, e0191530 (2018).

915 100. Duarte, E. H., Carvalho, A., López-Madrigal, S., Costa, J. & Teixeira, L. Forward genetics
916 in *Wolbachia*: Regulation of *Wolbachia* proliferation by the amplification and deletion of
917 an addictive genomic island. *PLOS Genet.* **17**, e1009612 (2021).

918 101. Woolfit, M. *et al.* Genomic evolution of the pathogenic *Wolbachia* strain, <i>w<i/>MelPop.
919 *Genome Biol. Evol.* **5**, 2189–2204 (2013).

920 102. Werren, J. H., Windsor, D. & Guo, L. R. Distribution of *Wolbachia* among neotropical
921 arthropods. *Proc R Soc Lond B* **262**, 197–204 (1995).

922 103. Martinez, J., Klasson, L., Welch, J. J. & Jiggins, F. M. Life and death of selfish genes:
923 comparative genomics reveals the dynamic evolution of cytoplasmic incompatibility. *Mol.*
924 *Biol. Evol.* **38**, 2–15 (2021).

925 104. Hoffmann, A. A., Hercus, M. & Dagher, H. Population dynamics of the *Wolbachia*
926 infection causing cytoplasmic incompatibility in *Drosophila melanogaster*. *Genetics* **148**,
927 221–231 (1998).

928 105. Reynolds, K. T. & Hoffmann, A. A. Male age, host effects and the weak expression or non-
929 expression of cytoplasmic incompatibility in *Drosophila* strains infected by maternally
930 transmitted *Wolbachia*. *Genet. Res.* **80**, 79–87 (2002).

931 106. Giordano, R., O'Neill, S. L. & Robertson, H. M. *Wolbachia* infections and the expression
932 of cytoplasmic incompatibility in *Drosophila sechellia* and *D. mauritiana*. *Genetics* **140**,
933 1307–1317 (1995).

934 107. Hoffmann, A. & Turelli, M. Unidirectional incompatibility in *Drosophila simulans*:
935 inheritance, geographic variation and fitness effects. *Genetics* **119**, 435–444 (1988).

108. Rousset, F. & Solignac, M. Evolution of single and double *Wolbachia* symbioses during speciation in the *Drosophila simulans* complex. *Proc. Natl. Acad. Sci.* **92**, 6389–6393 (1995).

109. James, A. C. & Ballard, J. W. O. Expression of cytoplasmic incompatibility in *Drosophila simulans* and its impact on infection frequencies and distribution of *Wolbachia pipientis*. *Evolution* **54**, 1661–1672 (2000).

110. Ballard, J. W. O. Sequential evolution of a symbiont inferred from the host: *Wolbachia* and *Drosophila simulans*. *Mol. Biol. Evol.* **21**, 428–442 (2004).

111. Bourtzis, K., Nirgianaki, A., Markakis, G. & Savakis, C. *Wolbachia* infection and cytoplasmic incompatibility in *Drosophila* species. *Genetics* **144**, 1063–1073 (1996).

112. Choi, J. Y., Bubnell, J. E. & Aquadro, C. F. Population genomics of infectious and integrated *Wolbachia pipientis* genomes in *Drosophila ananassae*. *Genome Biol. Evol.* **7**, 2362–2382 (2015).

113. Osborne, S. E., Leong, Y. S., O'Neill, S. L. & Johnson, K. N. Variation in antiviral protection mediated by different *Wolbachia* strains in *Drosophila simulans*. *PLOS Pathog.* **5**, e1000656 (2009).

114. Martinez, J. *et al.* Symbionts commonly provide broad spectrum resistance to viruses in insects: A comparative analysis of *Wolbachia* strains. *PLOS Pathog.* **10**, e1004369 (2014).

115. Gu, X. *et al.* A *w*Mel *Wolbachia* variant in *Aedes aegypti* from field-collected *Drosophila melanogaster* with increased phenotypic stability under heat stress. *Environ. Microbiol.* **24**, 2119–2135 (2022).

116. Ballard, J. & Melvin, R. Tetracycline treatment influences mitochondrial metabolism and mtDNA density two generations after treatment in *Drosophila*. *Insect Mol. Biol.* **16**, 799–802 (2007).

117. Cooper, B. S., Ginsberg, P. S., Turelli, M. & Matute, D. R. *Wolbachia* in the *Drosophila yakuba* complex: Pervasive frequency variation and weak cytoplasmic incompatibility, but no apparent effect on reproductive isolation. *Genetics* **205**, 333–351 (2017).

118. Canty, C. & Ripley, B. boot: Bootstrap R (S-Plus) functions. (2017).

119. R Core Team. *R: A Language and Environment for Statistical Computing*. (R Foundation for Statistical Computing, Vienna, Austria, 2023).

120. Bates, D., Mächler, M., Bolker, B. & Walker, S. Fitting linear mixed-effects models using lme4. *J. Stat. Softw.* **67**, 1–48 (2015).

121. Singmann, H., Bolker, B., Westfall, J., Aust, F. & Ben-Shachar, M. S. *Afex: Analysis of Factorial Experiments*. (2020).

122. Pfaffl, M. W. A new mathematical model for relative quantification in real-time RT–PCR. *Nucleic Acids Res.* **29**, e45–e45 (2001).

123. Schneider, C. A., Rasband, W. S. & Eliceiri, K. W. NIH Image to ImageJ: 25 years of image analysis. *Nat. Methods* **9**, 671–675 (2012).

124. Klasson, L. *et al.* The mosaic genome structure of the *Wolbachia w*Ri strain infecting *Drosophila simulans*. *Proc. Natl. Acad. Sci.* **106**, 5725–5730 (2009).

125. Salzberg, S. L. *et al.* Serendipitous discovery of *Wolbachia* genomes in multiple *Drosophila* species. *Genome Biol.* **6**, R23 (2005).

126. Ellegaard, K. M., Klasson, L., Näslund, K., Bourtzis, K. & Andersson, S. G. Comparative genomics of *Wolbachia* and the bacterial species concept. *PLoS Genet.* **9**, e1003381 (2013).

127. Seemann, T. Prokka: rapid prokaryotic genome annotation. *Bioinformatics* **30**, 2068–2069 (2014).

128. Höhna, S. *et al.* RevBayes: Bayesian phylogenetic inference using graphical models and an interactive model-specification language. *Syst. Biol.* **65**, 726–736 (2016).

129. Hoskins, R. A. *et al.* The Release 6 reference sequence of the Drosophila melanogaster genome. *Genome Res.* **25**, 445–458 (2015).

130. Hu, T. T., Eisen, M. B., Thornton, K. R. & Andolfatto, P. A second-generation assembly of the Drosophila simulans genome provides new insights into patterns of lineage-specific divergence. *Genome Res.* **23**, 89–98 (2013).

131. Conner, W. R. *et al.* A phylogeny for the *Drosophila montium* species group: A model clade for comparative analyses. *Mol. Phylogenet. Evol.* **158**, 107061 (2021).

132. Clark, A. G. *et al.* Evolution of genes and genomes on the *Drosophila* phylogeny. *Nature* **450**, 203–218 (2007).

133. Katoh, K. & Standley, D. M. MAFFT multiple sequence alignment software version 7: improvements in performance and usability. *Mol. Biol. Evol.* **30**, 772–780 (2013).

134. Revell, L. J. phytools: an R package for phylogenetic comparative biology (and other things). *Methods Ecol. Evol.* **3**, 217–223 (2012).

135. Boettiger, C., Coop, G. & Ralph, P. Is your phylogeny informative? Measuring the power of comparative methods. *Evolution* **66**, 2240–2251 (2012).

136. Suvorov, A. *et al.* Widespread introgression across a phylogeny of 155 *Drosophila* genomes. *Curr. Biol.* **32**, 111–123 (2022).

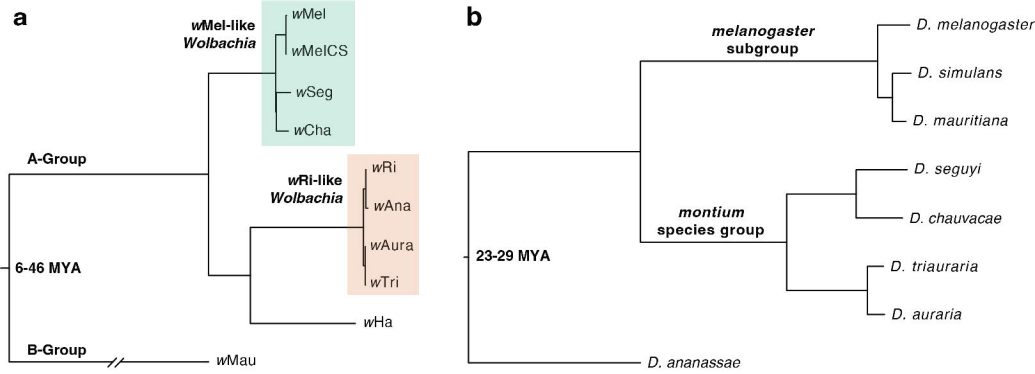
a
wMel-like
Wolbachia
wMel
wMelCS
wSeg
wCha
A-Group
wRi-like
Wolbachia
wRi
wAna
wAura
wTri
6-46 MYA
wHa
B-Group
wMau
b
melanogaster
subgroup
D. melanogaster
D. simulans
D. mauritiana
D. seguyi
D. chauvacae
montium
species group
23-29 MYA
D. triauraria
D. auraria
D. ananassae

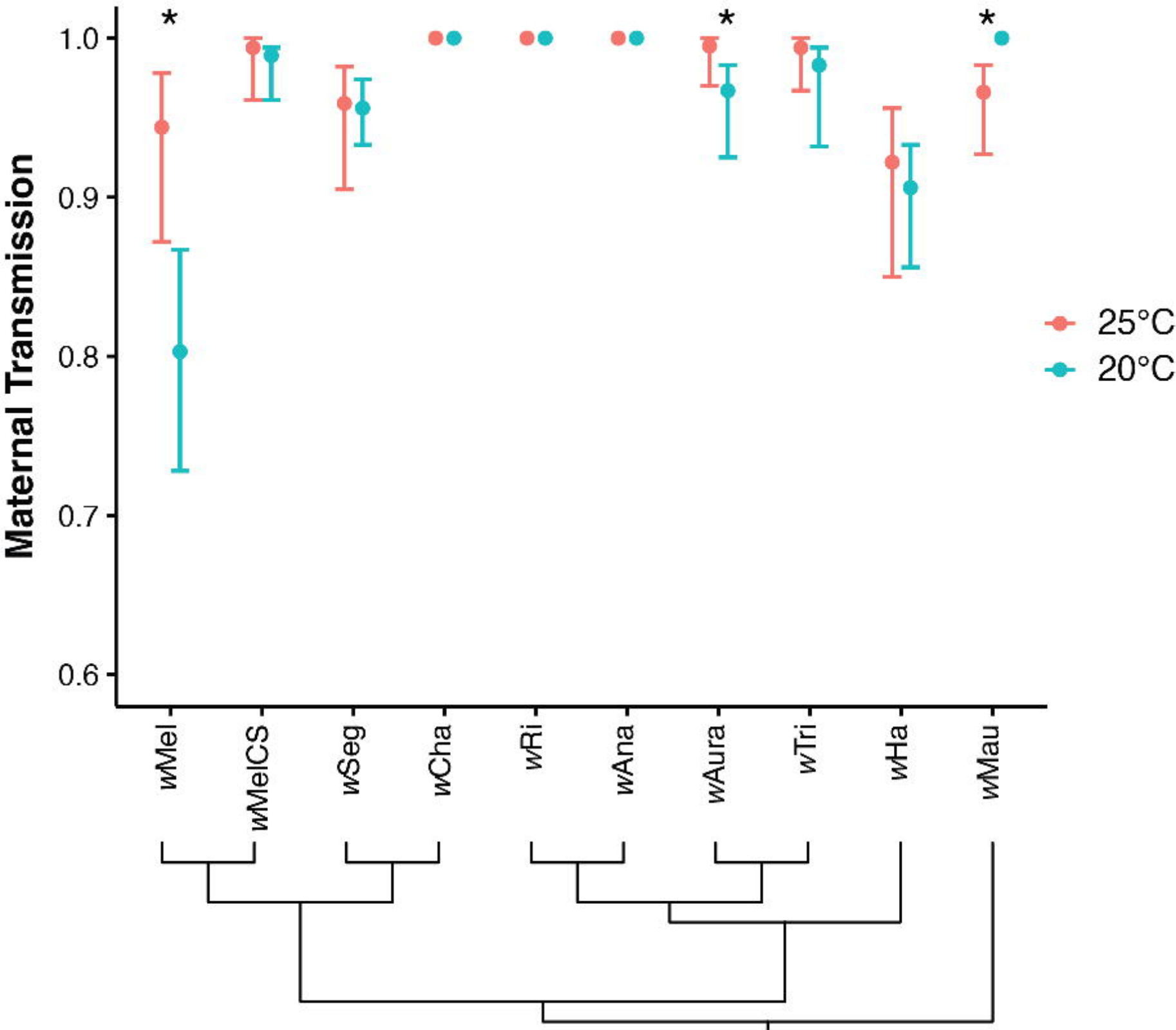
Maternal Transmission
1.0
0.9
0.8
0.7
0.6
*
*
*
25°C
20°C
wMel
wMelCS
wSeg
wCha
wRi
wAna
wAura
wTri
wHa
wMau

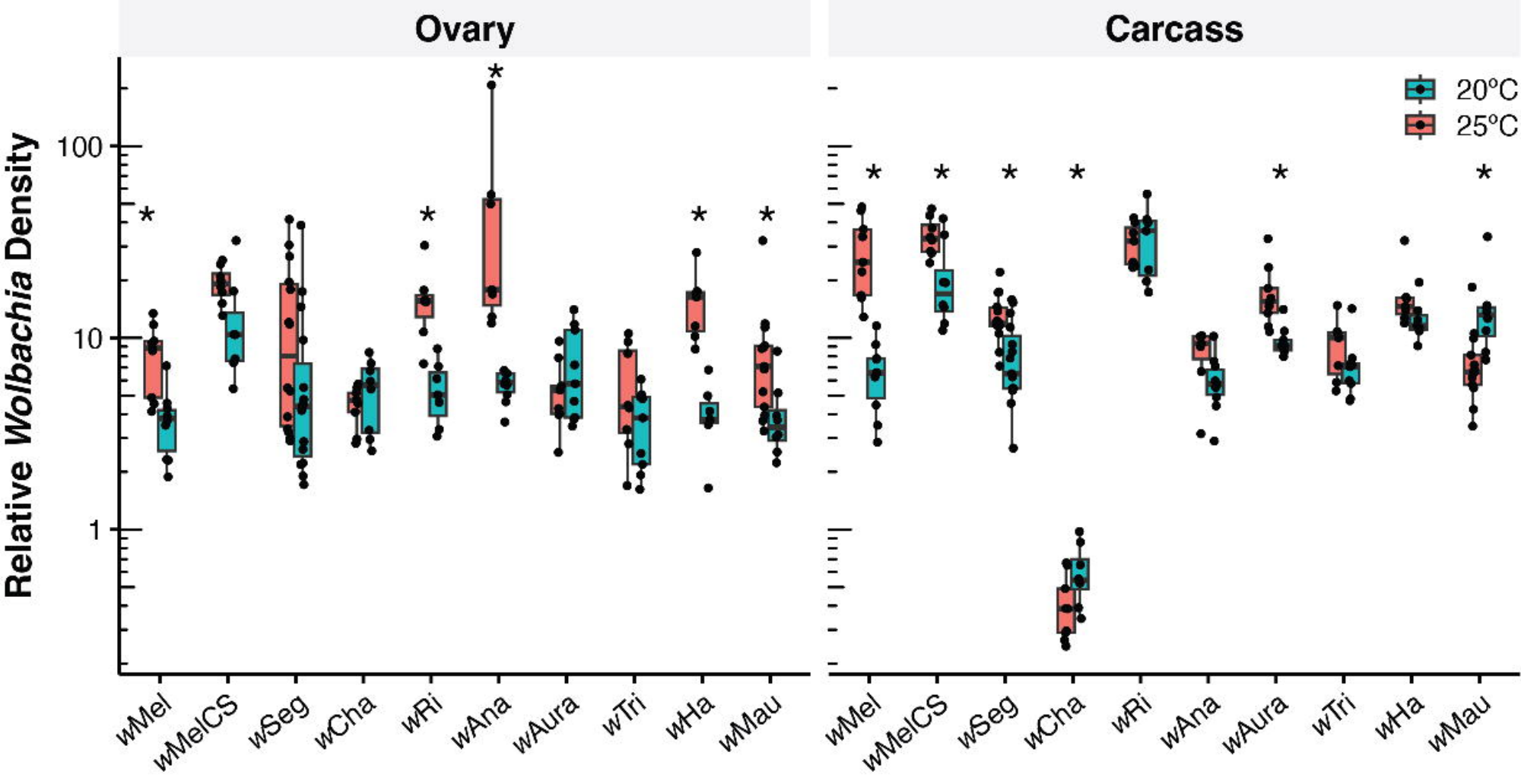
Ovary
Carcass
Relative Wolbachia Density
100
10
1
20ºC
25ºC
wMel
wMelCS
wSeg
wCha
wRi
wAna
wAura
wTri
wHa
wMau

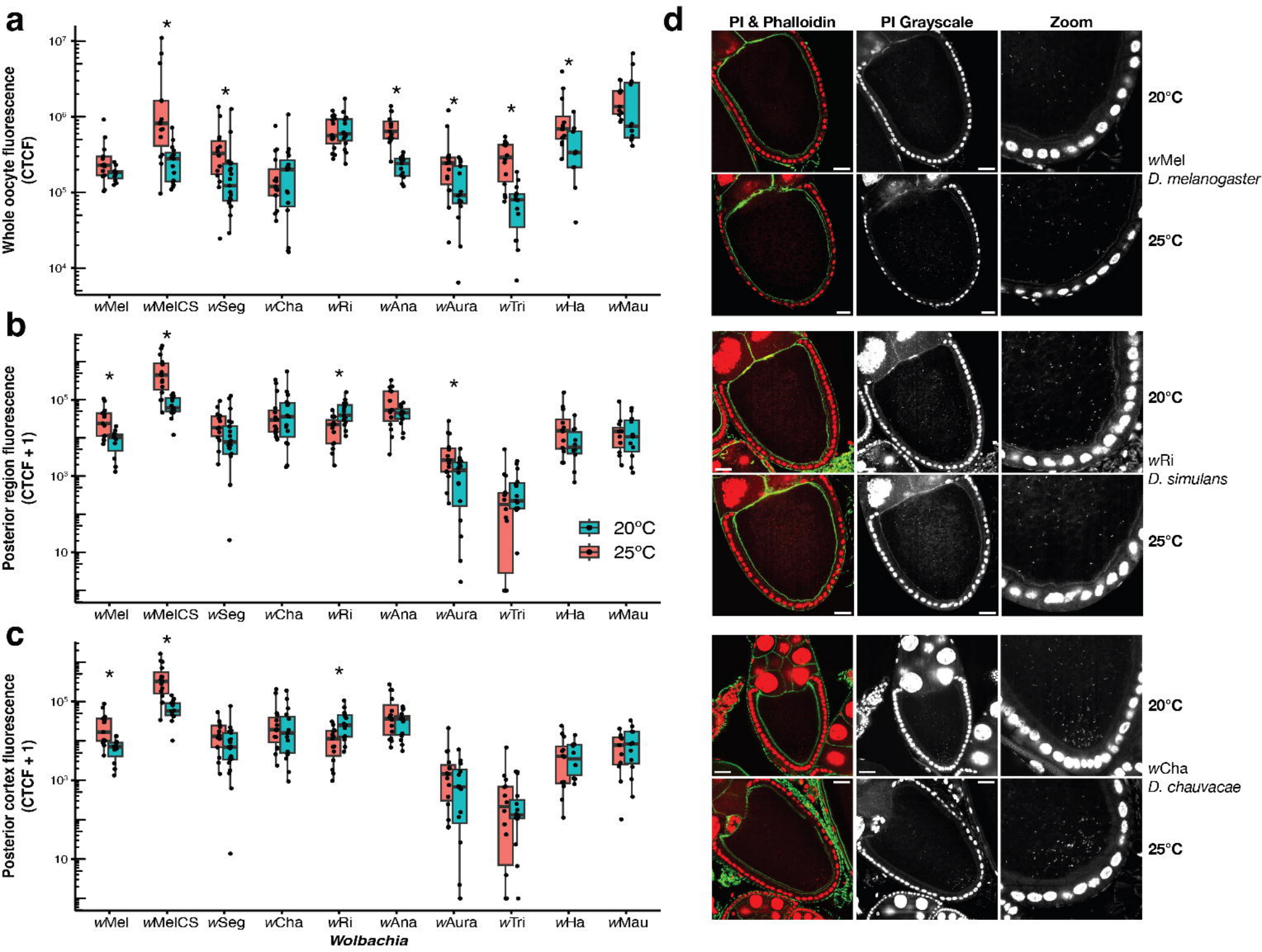
a
Whole oocyte fluorescence (CTCF)
b
Posterior region fluorescence (CTCF + 1)
c
Posterior cortex fluorescence (CTCF + 1)
wMel
wMelCS
wSeg
wCha
wRi
wAna
wAura
wTri
wHa
wMau
Wolbachia
20°C
25°C
d
PI & Phalloidin
PI Grayscale
Zoom
wMel
D. melanogaster
wRi
D. simulans
wCha
D. chauvacae